Applied Water Science (2023) 13:193
https://doi.org/10.1007/s13201-023-02000-6

ORIGINAL ARTICLE

Azadirachta indica-assisted green synthesis of magnesium oxide nanoparticles for degradation of Reactive Red 195 dye: a sustainable environmental remedial approach

Shumaila Kiran[1] · Hasan B. Albargi[2,3] · Gulnaz Afzal[4] · Ume Aimun[1] · Muhammad Naveed Anjum[1] · Muhammad Bilal Qadir[5] · Zubair Khaliq[6] · Mohammed Jalalah[3,7] · Muhammad Irfan[7] · M. M. Abdullah[2,3]

Received: 22 June 2023 / Accepted: 13 August 2023 / Published online: 8 September 2023

Abstract

A variety of industries employ synthetic azo dyes. However, the biosphere is being damaged by the unused/leftover azo dyes, which pose a danger to all living things. Therefore, treating them to shield the environment from the potential harm of azo dyes is crucial. Bio-sorption is a cheap and effective mode for eliminating toxic dyes in the environment. The current work focused on synthesizing magnesium oxide (MgO) nanoparticles using an aqueous leaf extract of neem (*Azadirachta indica*). The XRD and SEM analyses of MgO nanoparticles indicated the crystalline nature of MgO nanoparticles with a cubic structure, and the size was around 90–100 nm. FTIR analysis showed the presence of a stretching frequency peak at 550 cm^{-1}, confirming the Mg–O bond. The surface analysis revealed the cluster form of the synthesized nanoparticles. The UV–visible absorption peak for MgO nanoparticles was found at 294 nm and band gap of 4.52 eV. In order to eliminate the Reactive Red 195 dye, MgO nanoparticles were used. At pH 4, 40 °C, 0.02% dye concentration, and 0.003 g/L catalyst amount, the highest degree of decolorization (91%) was seen. Decreased total organic carbon (TOC) and the chemical oxygen demand (COD) percent were 84.33% and 81.3%, respectively. The proposed mechanism of target dye degradation was also investigated. MgO NPs were found to be effective in their catalytic behavior toward the degradation of Reactive Red 195 dye up to five cycles with almost no change in their catalytic activity.

Keywords Greener approach · MgO nanoparticles · Nanotechnology · Reactive Red 195 dye remediation · COD · TOC

✉ Shumaila Kiran
shumaila.asimch@gmail.com

✉ Hasan B. Albargi
hbalbargi@nu.edu.sa

1 Department of Applied Chemistry, Government College University, Faisalabad 38000, Pakistan

2 Department of Physics, Faculty of Science and Arts, Najran University, 11001 Najran, Saudi Arabia

3 Promising Centre for Sensors and Electronic Devices (PCSED), Advanced Materials and Nano-Research Centre, Najran University, 11001 Najran, Saudi Arabia

4 Department of Zoology, The Islamia University of Bahawalpur, Bahawalpur, Pakistan

5 Department of Textile Engineering, National Textile University, Faisalabad 37610, Pakistan

6 Department of Materials, National Textile University, Faisalabad 37610, Pakistan

7 Department of Electrical Engineering, College of Engineering, Najran University, 11001 Najran, Saudi Arabia

Introduction

Water is a primary and highly essential component of the ecosystem. Industrial and house wastewaters contain toxic and deadly chemicals threatening human well-being and the environment (Zhao et al. 2019). Numerous stages of the textile sector, like primary processing, use extensive water (Kiran et al. 2017). Because of the color, high chemical contents, biological oxygen needs, inorganic compounds, suspended particulate salts, total dissolved solids, and hazardous substances, wastewater from the textile sector is particularly problematic (Gulzar et al. 2017; Kiran et al. 2017). In addition, topical pollutants, known as azo dyes (such as Reactive Red 195 dye), concern water supplies because they build up in water so that light cannot reach the underground water surface, hindering plant growth. Azo dyes are used to dye cellulosic, wool, and silk materials (Leyla et al. 2012). The dyed wastewater is discarded into water streams without proper treatment, contributing to environmental pollution.

In addition, azo dyes reduce the water oxygen concentration causing marine life and plant mortality (Rafique et al. 2022).

It is pretty concerning because the azo dyes will eventually be released into water bodies, where they would damage the land, aquatic ecosystem, and subsurface water. Once these azo dyes enter the environment, their toxicity cannot be controlled effectively. Artificial colors pose serious health risks and significantly contribute to environmental degradation. Several organic dyes cannot break down easily because of their intricate aromatic nature (Bhatti et al. 2008). Because they contain hazardous, non-degradable pollutants absorbed by surface water, sediment, and soil, textile effluents are regarded as the primary industrial concerns (Yaseen and Scholz 2019). In Pakistan, wastewater from the textile industry is typically used as irrigation for growing crops. Researchers looking to make it easier for their recycling in the irrigation process or reuse inside the textile plant have focused increasingly on the treatment of these effluents due to the continued water shortage problem (Bhuiyan et al. 2016). Hence, it is essential that the frequently used azo dyes for various textile operations should be treated before their final disposal into the water system. Researchers have developed multiple techniques to remove such pollutants from water. Filtration (Khandaker et al. 2020), electroplating (Chen et al. 2020), membrane filtration (Hube et al. 2020), ion exchange process (Yan et al. 2020), adsorption (Zhou et al. 2019; Pang et al. 2023), and the use of nanoparticles (NPs) (Vaiano et al. 2018) are some of the different approaches that can be used to treat wastewater. The choice of an effective procedure for waste eradication is made more difficult by dyes' non-biodegradable constitution and resilience against oxidizing chemicals (Mahmoodi 2013a). Among these wastewater treatment techniques, the utilization of NPs is quite intriguing and may be a unique technique with several potentials for treating wastewater (Naseer et al. 2016). This is due to these NPs remarkable electric, mechanical, visual, and physicochemical features (Nezhadheydari et al. 2019).

The design of novel catalysts at the nanoscale has become a thriving area of study and invention (Erumpukuthicka et al. 2011). Metal or metal oxide NPs are gaining distinction due to distinct properties like porosity, smaller size, adsorbents, reducing agents, higher surface area, etc. (Kargozar and Mozafari 2018; Tyagi et al. 2018; Li et al. 2023). They exhibit unique physicochemical characteristics due to their strong reactivity, crystal form, substantial surface area, and nano-size effect. Therefore, NPs can combine with environmental pollutants and heavy metals and convert them into the simplest products (Yu et al. 2019). NPs can be synthesized by three methods, e.g., chemical, physical, and bio-based synthesis (Kumar et al. 2013; Kiran et al. 2018). Despite their popularity, their benefits are limited by their heavy price and the frequent presence of toxic ingredients (such as solvent, reducing agent, and other chemicals) that might pose serious dangers to health and the environment. On the other hand, biological methods are nontoxic, highly efficient, simple to use, and most significantly, environmentally beneficial (Kumar et al. 2013; Bauzar et al. 2016; Zhang et al. 2020). Recently, several research groups have successfully synthesized NPs via extracts obtained from single-celled creatures, such as microorganisms as well as from the extracts of plant materials (Duran et al. 2011; Gholizadeh et al. 2018; Rezazadeh et al. 2020). The biomolecules in the plants give the emerging nanostructures new characteristics and wonderful qualities (Makarov et al. 2014). The production of numerous metals, and their oxides, nitrides, etc., is a biologically sustainable process. There is a dire need for such procedures using medically secure, environmentally harmless ingredients and available options to reduce or eliminate the costlier ways and the environmentally damaging means in the synthetic sector (Ikram et al. 2015, 2020; Nabi et al. 2022; Sepahvand et al. 2020).

Magnesium oxide (MgO) is a significant metal oxide because of its exceptional and distinctive electrical, heating, visual, mechanical, and chemical features (Fakhri and Adami 2014). MgO, a cheap metal oxide employed as a skilled accelerator in various organic conversions, has been used in commercial nanotechnology applications (Baharfar and Shariat 2014; Safaei et al. 2015). MgO nanoparticles (MgO NPs) possess an increased effective surface area, crystalline morphological characteristics, and highly activated sites. As a result, MgO NPs are utilized in various fields, like in catalysis, food goods, paints, superconductors, antibacterial agents, photonics, sensor systems, and adsorbent materials (Abdukhaleq et al. 2020; Fouda et al. 2021; Saied et al. 2021; Sofi et al. 2021). Now, greener technologies that synthesize nanoparticles from natural origins like plants or plant extracts have been found as worthwhile substitutes for chemical processes. The addition of phytochemicals increases the antimicrobial property of MgO nanoparticles made from plant leaves extract (Bauzar et al. 2016; Aqeel et al. 2020). However, considering their diminutive stature and great sensitivity, NPs can penetrate consumable items via incorrect dumping in soil and water, which might harm one's health. In some previous studies, the cytotoxicity of MgO NPs has been established. For example, researchers found that the toxicity of MgO NPs caused cellular death in zebrafish embryos (Shah et al. 2015). Though MgO NPs toxicological consequences have been documented, their adverse effects have not yet been shown to be fatal; therefore, they are currently frequently used in various fields (Di et al. 2012).

Azadirachta indica (Neem) belongs to *Meliaceae* family and tropical and subtropical contexts, including Pakistan, Nepal, Bangladesh, Sri Lanka, and India (Asefi et al. 2010; Anumol et al. 2011). The phytochemicals present in

Neem are nimbin, catechins, salannin, azadirachtin, cyclic trisulfide, cyclic tetrasulfide, and flavanones (Revathi and Thambidurai 2018; Venkataravansppa et al. 2018). Neem contains flavonoids, which are significant phytonutrients. Flavonoids are essential for anchoring nanoparticles and function as encapsulating and reducing agents (Verma et al. 2016; Roy et al. 2017). Using bio-based synthesized MgO NPs to clean contaminants from polluted water is efficient (Sathish et al. 2022). With the least amount of energy and basic materials wasted, the invention of greener synthetic processes utilizing sustainable and environment-friendly materials, chemicals, and nontoxic agents is strongly advised (Patil et al. 2022; Sun et al. 2023).

Neem leaves are enriched with polyphenols (flavonoids), which act as reducing and capping agents. Hence using the neem leaves plant extract, there is no need to use chemical reducing agents, so it minimizes the number of chemicals for synthesizing MgO nanoparticles, making this approach sustainable and inexpensive. In this direction, we planned to work on synthesizing MgO NPs utilizing the neem leaf extract, followed by their characterization. MgO nanoparticles were then employed to remediate Reactive Red 195 (RR-195) dye. Reactive Red 195 dye was used as a model azo dye to optimize the reaction conditions at the laboratory level, so these optimal conditions can be effectively applied at the industrial level to remediate polluted water effectively. The optimal conditions were then applied to textile effluent to check the effectiveness of the studied method at the industrial level.

Materials and methods

The Reactive Red 195 dye (structural shown in Fig. 1) was purchased from Chaudhary Dyes and Chemicals in Faisalabad, Pakistan (Table 1).

The complete experimental layout is given in Fig. 2.

Sample collection and preparation

Neem (*Azadirachta indica*) leaves were gathered from the Punjab Forest Department in Faisalabad, Pakistan. Initially, the leaves were carefully washed with tap water and then distilled water to remove dirt and other things stuck to the leaves' surface. Next, the leaves were air-dried. Leaf extract was prepared by steaming about 30 g of fine leaves powder in 300 mL of distilled water at 50 °C for 25 min. A yellow-colored solution was formed. The extract was stored for seven days in the fridge after being filtered by Whatman filter paper no. 1 (Nguyen et al. 2021).

Table 1 Characteristics of Reactive Red 195 dye (target dye)

Color index (C.I) name	M (g/mol)	λ_{max}	Solubility	Chemical structure
Reactive Red 195	1168	540 nm	Soluble in water	See Fig. 1

Preparation of magnesium oxide nanoparticles

In a reaction vessel, leaf extract (5 mL) and distilled water (20 mL) were mixed and heated to 60 °C. Five grams of $Mg(NO_3)_2$ was introduced into it, and the reaction solution was heated at 70 °C with constant stirring. The formation of MgO NPs could be visualized by transforming the solution's color from yellow to brown. The synthesized MgO NPs were

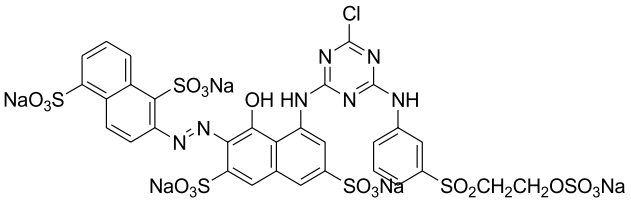

Fig. 1 Structure of C.I. Reactive Red 195 dye (C.I. 93,050–79-4)

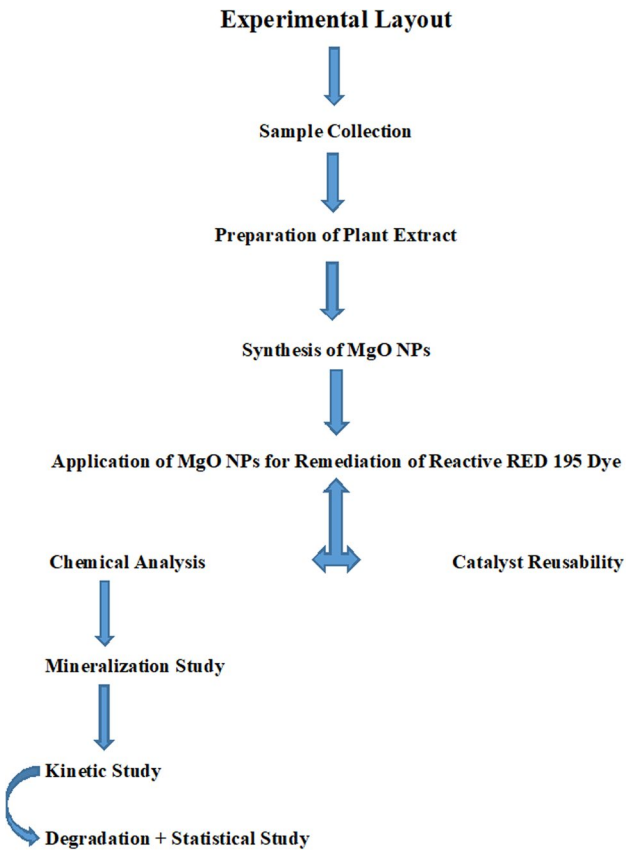

Fig. 2 Experimental layout

centrifuged at 10,000 rpm for 10 min to remove impurities, and then, the pellet was re-dispersed in distilled water. Then, ethanol was used to clean the MgO NPs of contaminants before they were processed for a day at 45–50 °C (Kiran et al. 2018). The extract solution is supplemented with polyphenols, which help to stabilize metal salt nanoparticles as a stabilizing agent and also help to reduce them into nanoparticles (Elumalai et al. 2015; Moavi et al. 2021). The whole procedure is picturized in Fig. 3. The possible interactions that occur during the manufacture of MgO nanoparticles between the bio-organic molecules and magnesium salt are given in Fig. 4.

Characterization of magnesium oxide nanoparticles (MgO NPs)

The prepared MgO NPs were identified by UV–visible and FTIR spectral analyses, SEM and XRD.

Application of MgO nanoparticles to clean up the Reactive Red 195 dye

Scanning of λ_{max}

For scanning of λ_{max}, absorbance values were measured. For this purpose, a series of dilutions of dye solution was prepared, and with the help of a UV–visible spectrophotometer, absorbance was calculated.

Experimental procedure

MgO NPs (1 mg) were introduced to the reactive dye solution (10 ppm) in the reaction container. The pH was kept constant until 4 by adding 1 M NaOH/ 1 M HCl. After it, for 90 min, the reaction container was held on a hot plate at 50 °C with a magnetic stirrer. A little aliquot was removed from the reaction's solution to check its absorbance after every 15 min using a UV–visible spectrophotometer (Kiran et al. 2018).

Optimization of experimental factors

Various reaction parameters such as dose of dye (0.01–0.05%), the amount of MgO NPs (1–5 mg), pH (4–9), and temperature (30–70 °C) parameters were optimized similarly as mentioned above. The other variables were held fixed, while one changed at a time.

Fig. 3 Multiple phases in the preparation of MgO NPs by neem leaves extract: (**a**) extract preparation and (**b**) synthesis of MgO NPs

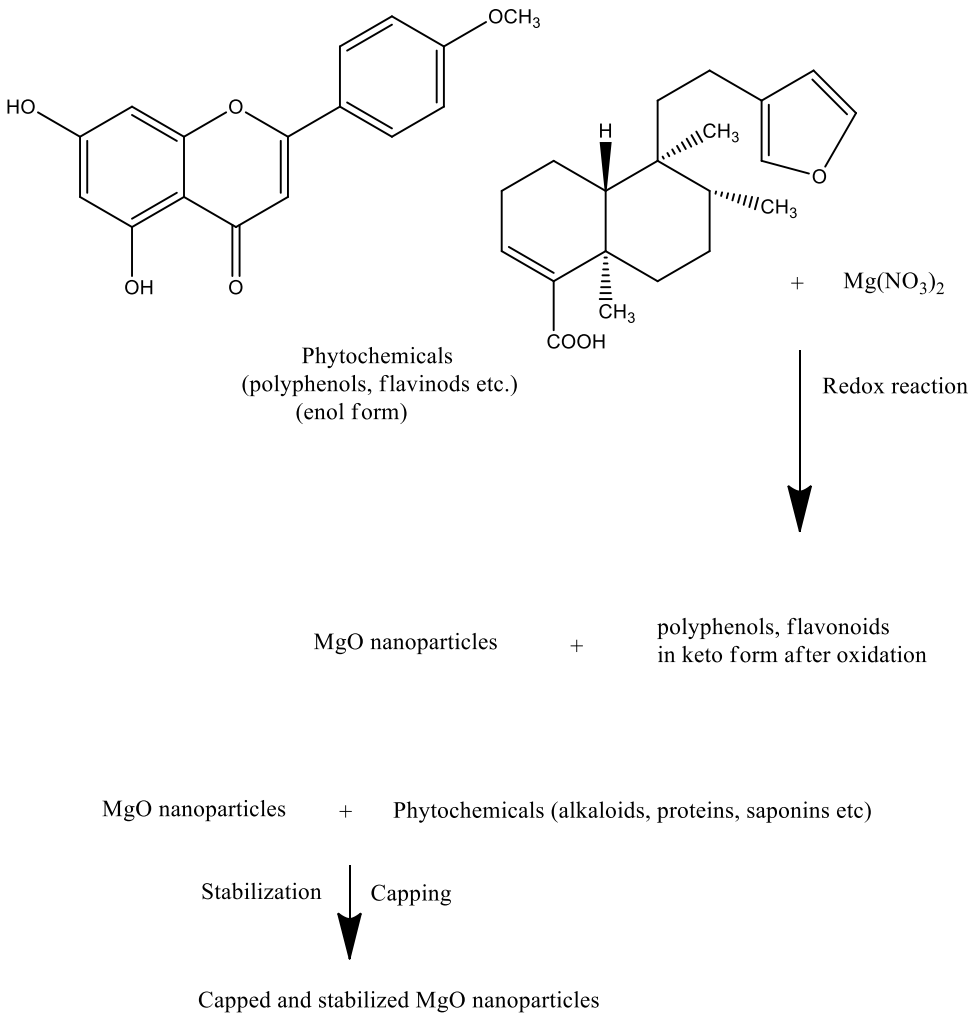

Fig. 4 Interactions that occur during the manufacture of MgO nanoparticles between the bio-organic molecules and magnesium salt

Chemical analysis

Every experiment was run three times for the confirmation of the results. The absorbance was observed at λ_{max} (540 nm) using a UV–visible spectrophotometer. The effective percent decolorization of all parameters was estimated by measuring the solution absorbance. The equation given below was applied to get the percentage of decolorization:

$$Decolorization\ (\%) = \left[(I - F)/I\right] \times 100 \quad (1)$$

Here I is the initial absorbance at zero time, and F is the final absorbance of the dye solution.

Treatment of textile ındustrial effluent

In this part, the conditions were optimized using Reactive Red 195 dye as a model dye and applied on textile effluent to check the effectiveness of MgO nanoparticles at the industrial level. The same method was adopted outlined above for Reactive Red 195 dye. The decolorization efficiency is calculated using Eq. 1..

Mineralization study and kinetics study

Samples of dye (both treated and untreated) were assessed by estimating various parameters like COD and TOC values (Moorthy et al. 2015). The kinetics of the reaction was studied to find the order of the reaction.

Catalyst reusability

In this study's optimal conditions, the catalyst's reusability was investigated. The reaction specimens were spun at 2000–4000 rpm for 15 min or as soon as the catalyst accumulated near the tube's bottom. Three acetone washes were performed on the deposited catalyst to eliminate all organic residues before it was employed in another catalyzed reaction. After every round of the reaction, the catalyst was

separated and reused using the same procedure, and catalyst efficiency toward target dye decolorization was calculated.

Degradation study and statistical analysis

The degradation of the target dye was evaluated in several phases, with rupturing of old bonds and the creation of fresh, simple compounds (Suresh et al. 2014; Kiran et al. 2018). The results were computed by finding the standard error of means (Greenberg 1985).

Results and discussion

Characterization of MgO nanoparticles

Analysis using UV–visible spectroscopy

Figure 5a depicts the UV–Vis absorption spectrum for MgO nanoparticles from 200 to 800 nm. MgO nanoparticles made in a biogenic way showed a characteristic absorption peak at 294 nm. Tauc's equation was employed to find the band gap of magnesium oxide.

$$(\alpha h\nu) = A(h\nu - Eg)^n \quad (2)$$

where n is a constant equal to ½ for the direct band gap, h is Planck's factor, A is a fixed value, E_g is the bandgap energy, and α is the absorption coefficient. Using extrapolation from the line, the band gap of the MgO nanoparticles is determined from Fig. 5b. The symbol A represents the optical absorption factor, while v stands for frequency. It was discovered that the bandgap was about 4.52 eV after extrapolating the graph.

FTIR analysis

MgO nanoparticles were also characterized by FTIR analysis. Three characteristics were observed. One peak was at 3455 cm^{-1} for the –OH group; one peak at a stretching frequency of 1375 cm^{-1} for the C = O group demonstrates an aromatic ring's presence, and one peak at 550 cm^{-1} is characteristic of the Mg–O bond (Fig. 6).

SEM and XRD analyses of MgO nanoparticles

SEM and XRD analyses were conducted to examine the MgO NPs' shape and diameter. This gives information about the nanoparticles' shape and size. The illustration beneath shows purified MgO nanoparticles as delicate, tiny, unified groupings with a spherical shell shape. MgO NPs were identified in an aggregate form (Fig. 7). An X-ray diffraction study was conducted to determine whether the MgO nanoparticles were crystallized or amorphous. It took the use of a sample material of MgO nanoparticles. XRD revealed our MgO NPs to be semicrystalline (Fig. 8). The results show that the MgO nanoparticles are in cubic phases with a

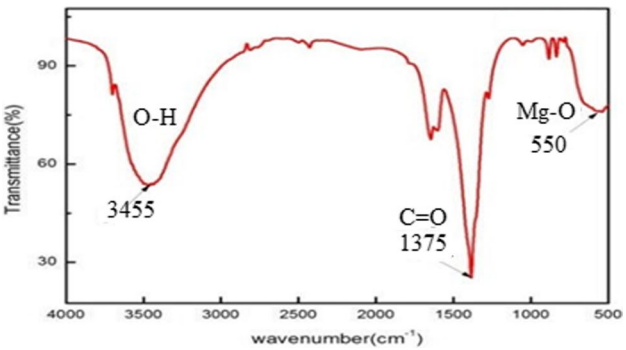

Fig. 6 FTIR spectrum of magnesium oxide nanoparticles

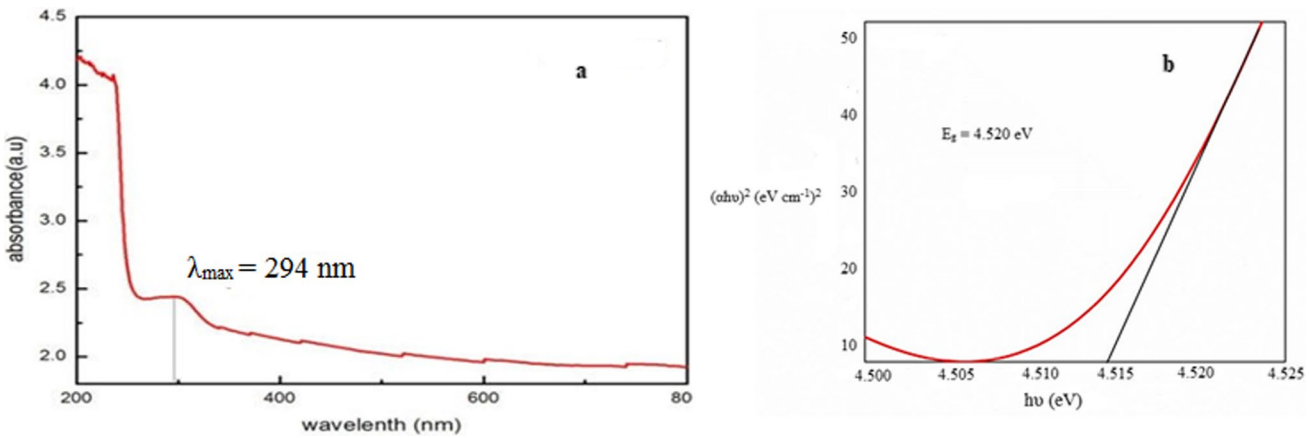

Fig. 5 UV–visible absorption spectrum: (**a**) band gap and (**b**) of magnesium oxide nanoparticles

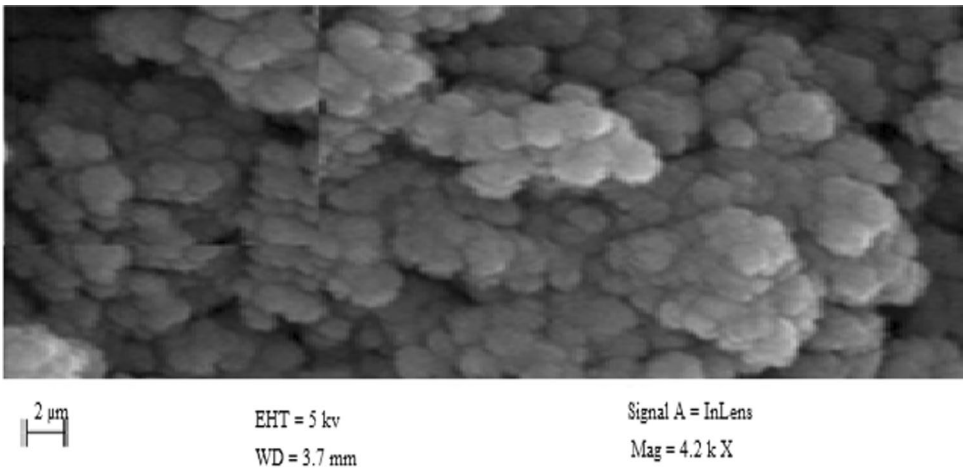

Fig. 7 SEM photograph of MgO nanoparticles

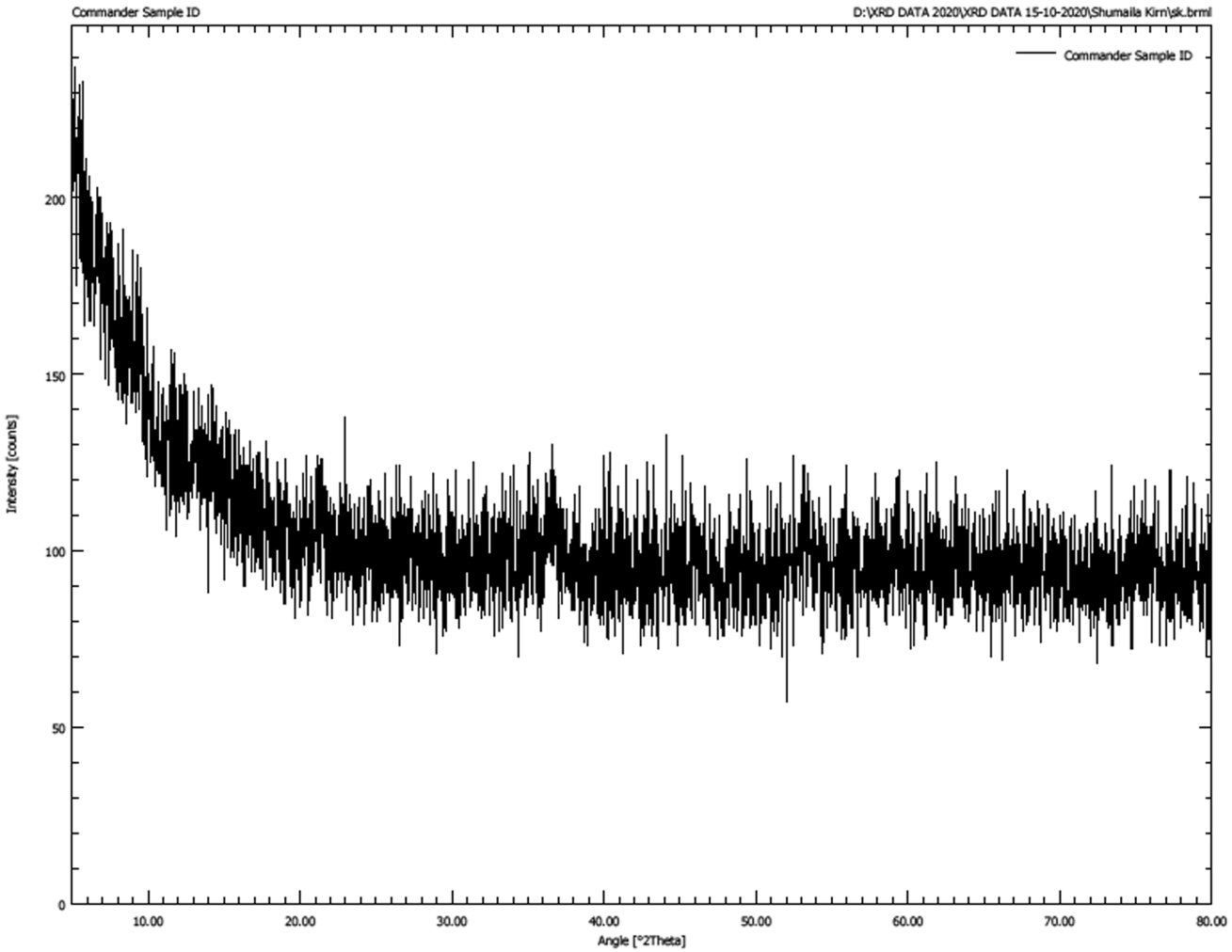

Fig. 8 XRD image of MgO NPs

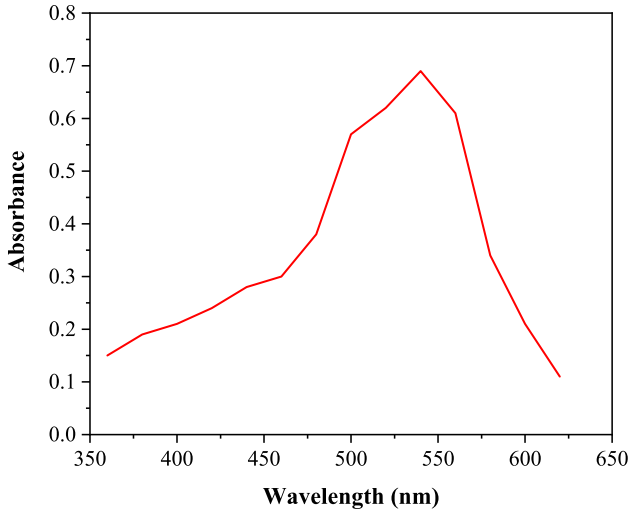

Fig. 9 Determination of λ_{max} by maximum absorbance for Reactive Red 195 dye

mean crystallite diameter of almost 90–100 nm and do not contain any impurity phases (Kandiban et al. 2015; Aravind et al. 2016).

Determination of λ_{max} for Reactive Red 195 dye

The absorbance value was scanned from 360 to 640 nm, with a pause of 20 nm wavelength to determine the wavelength of the highest absorption value. Figure 9 indicates that the λ_{max} is 540 nm.

Optimization of experimental conditions for decolorization of Reactive Red 195 dye

Effect of dye dose The concentration of a dye is a significant factor in its treatment using an appropriate catalyst. The influence of several initial dye concentrations on catalytic degradation is evaluated from 0.01 to 0.05%. The decolorization increased as the starting amount of dye rose from 13.4% to 68.5% in 75 min. The maximum decolorization has occurred at a concentration of 0.02% (Fig. 10a). Up until a certain level, a rise in the amount of dye causes a rise in dye absorption on the catalyst's surface, and the reaction may be retarded with a further rise in dye level (Ghaffar et al. 2021). It results from the competition between dye particles for binding on the catalyst's outermost layer, thereby decreasing the number of active locations readily accessible for the catalytic reagent (Raza et al. 2020). By increasing dye concentration, the dye particles start acting as an inhibitor, which reduces catalytic activity (Kiran et al. 2018). When more dye particles are present, self-association and clumping can result, which prevents dye particles from reaching the available catalytic region and lowers the reaction rates (Venkataravanappa et al. 2018; et al. 2018; David et al. 2020; Gola et al. 2021; Elashery et al. 2023).

Effect of catalyst dose The amount of the catalyst and aggregation of catalyst particles in high amounts also influence the decolorization of dye. Digestion of dye increases with increasing catalytic concentration, which is a feature of heterogeneous catalysis. Simply raising the catalyst concentration results in more active areas of the catalyst. A sequence of experiments was conducted using MgO NPs of various concentrations (0.001, 0.002, 0.003, 0.004, and 0.005 g) to find the most appropriate catalytic dosage. It has been observed that the percentage decline has elevated from 4.2% to 62.4%. Above the 0.003 g amount of MgO NPs, the rate of dye decolorization has not significantly increased. Therefore, 0.003 g/L of MgO NPs has been considered a suitable dose for decolorizing Reactive Red 195 dye (Fig. 10b). However, increased catalyst levels may result in turbidity look in its solution (Mahmoodi 2013b; Elashery et al. 2023). The rising decolorization value with increased catalyst quantity leads to accelerated growth throughout the energetic surface region. Over a certain amount of catalyst, the reaction rate decreases as the catalyst's binding sites, which were previously responsible for increasing the reaction rate, become fewer in number (Mhmoodi et al. 2014; Tahir et al. 2023). Additionally, the response products are likely to degrade the catalytic effectiveness at its increased level, which will slow the reaction rate (Kamranifar et al. 2018; Prabhu et al. 2023). Furthermore, the reaction products may interfere with the catalyst's efficacy in its larger amount, which could cause the process to slow down or cease (Rafique et al. 2018; Mahmoodi et al. 2019; Foster et al. 2019; Kiran et al. 2022; Rasool et al. 2023).

Effect of pH There were tests done at varying pH levels from 4 to 9. The highest dye removal (75.5%) value was observed at pH 4 using MgO nanoparticles as a catalyst, as shown in Fig. 10c. The rate of dye decolorization decreased when pH rose from 5 to 9. As a result, pH 4 was the ideal value for the decolorization of the dye in the investigation. The dye solution's pH has a significant influence on the efficacy of dye removal. Even a tiny pH shift can considerably affect the reaction's rate. Because of this, pH optimization is a crucial factor (Rafique et al. 2018). The MgO NPs surface can be protonated or deprotonated under the acidic or alkaline medium (Rafique et al. 2021; Wang et al. 2021, 2022). Beyond a certain pH, a catalytic agent may accomplish no discernible decolorization (Khalid et al. 2013). The findings of the experiment agreed with the literature (Sattar et al. 2010; Ahuja et al. 2016; Lourens et al. 2023).

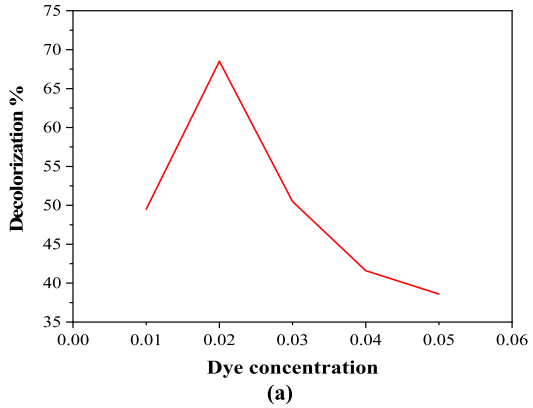

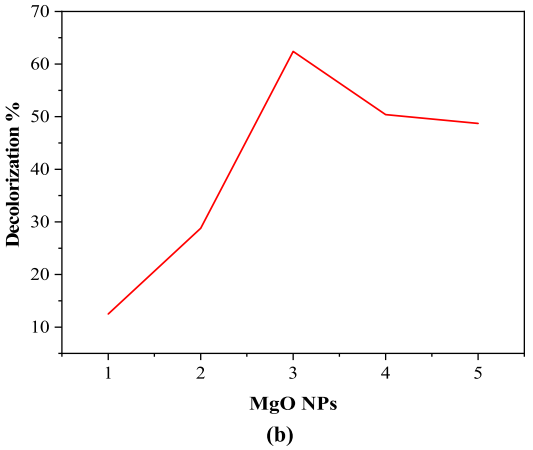

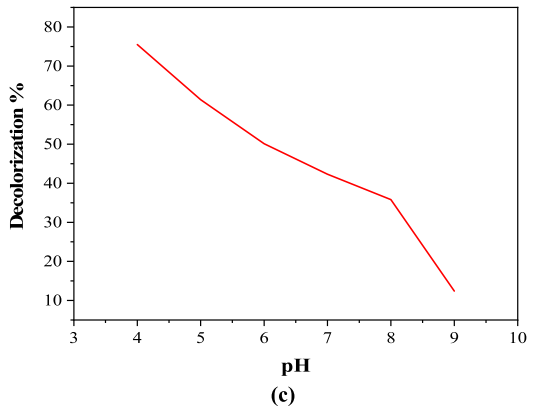

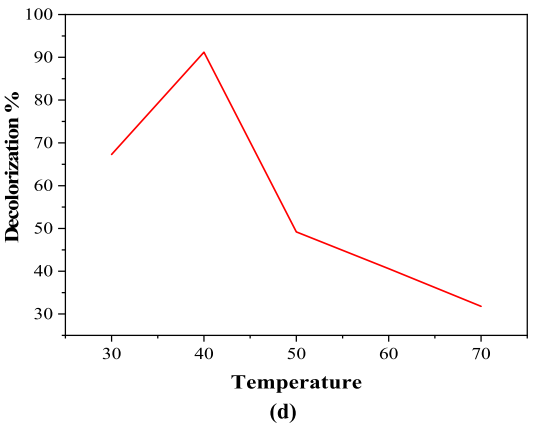

Fig. 10 Effect of (**a**) dye concentration, (**b**) MgO nanoparticles concentration, (**c**) pH (**d**) temperature on decolorization (%) of Reactive Red 195 dye using MgO nanoparticles

Effect of temperature The temperature effect on the decolorization of Reactive Red 195 dye was calculated at 30–70 °C. The experiments were left to run for 90 min. The maximum decolorization (91.2%) was seen at 40 °C (Fig. 10d). Reactive Red 195 dye's decolorization effectiveness in this treatment method was gradually decreased as the temperature rose (Kiran et al. 2020). At higher temperatures, the adsorption capacity is reduced, and this was likely as a result of the procedure of sintering and temperature increase, which results in the reduction in surface area of the catalyst for alteration in the catalyst's three-dimensional shape, which may hinder the active binding of substrate, resulting in decreasing the reaction rate (Kiran et al. 2018; Khalil et al. 2021). It could be because the sintering process with increased temperature leads to a reduction in the catalytic surface, which lowers the catalyst's ability to adsorb substances (Lafta 2015; Mohammad et al. 2016). The attachment of dye particles to the catalytic surface is typically retarded by a higher temperature because this could change the three-dimensional orientation of nanoparticles (da Silva et al. 2019; Jaina et al. 2023).

Application of optimized conditions for treatment of textile effluent

The experiments were conducted at the optimized experimental conditions (pH 4, MgO NPs dose 3 mg; temperature 40 °C, time 50 min) of catalytic treatment using Mg-NPs as a catalyst to determine the decolorization potential of textile industrial effluent. The textile effluent was decolorized (85.1%) by Mg-NPs as a catalyst (Fig. 11) but showed less decolorization (%) potential as was observed for Reactive Red 195 dye (91%) by the same treatment. Rezaee et al. (2008) employed the photo-Fenton method to decolorize textile wastewater containing various reactive dyes and reported that the effluent could be decolored up to 80%. According to Rocher et al. (2008), the dye decolorization process relies mainly on the dye's characteristics and the adsorbent. As a result, MgO NPs exposure with higher decolorization percentages may result in the adsorption of tiny dye molecules on their surface (Jindarom et al. 2007; Fouda et al. 2021; Aziz et al. 2023). According to Nga et al. (2013), the electrostatic interaction among the negatively charged particles of the dyes and the positive charges of the sites for adsorption on the outer layer of NPs is the cause of the elimination of dye color caused by NP treatment.

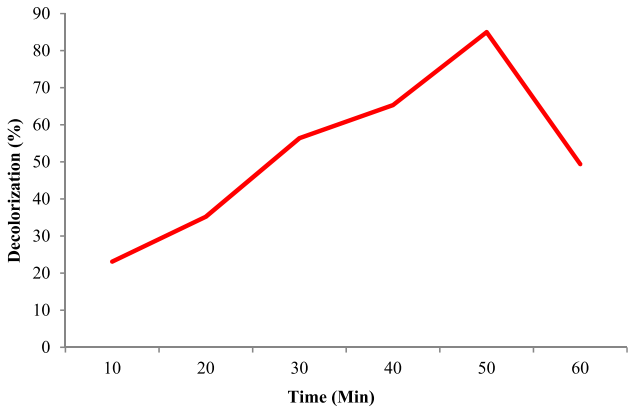

Fig. 11 Effect of catalytic treatment of MgO nanoparticles on decolorization of textile Industrial effluent at optimized conditions

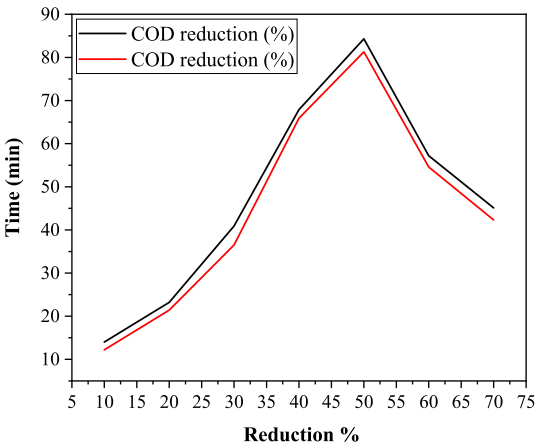

Fig. 12 Effect of catalytic period of interaction on water quality factors

Measurement of quality assurance parameters

The effectiveness of quality standards like COD and TOC was investigated by MgO nanoparticles. It was shown that the elimination (percent) of the two water quality measures increased as the response time increased during the evaluation of TOC & COD of the treated Reactive Red 195 dye sample. The COD and TOC (in percent) decline was reported to be 84.33 and 81.3, respectively (Fig. 12). Therefore, it could be inferred that MgO NPs ensure dye breakdown by lowering COD and TOC of the solution in addition to removing color. The fact that both values have decreased by a certain percentage shows that our dye molecule was decolored and destroyed. The literature also supports these findings (Mahmoodi et al. 2018; Sela et al. 2020).

Kinetics study

Different methods can study dye degradation. One of the important ways to describe the degradation of Reactive Red 195 dye against catalyst dosage (MgO NPs) is received by applying kinetic interpretation to determine the order of dye degradation reaction. For this purpose, a linear data fitting model (LDFM) was applied to the Reactive Red 195 dye decolorization spectrometric data against the catalyst for the execution of results that make the reaction order clear (Mahmoodi et al. 2007; Mahmoodi et al. 2010; Mahmoodi et al. 2015).

Figure 13a shows that the graph is plotted between dye conc. on the y-axis and time on the x-axis. Figure 13a shows different dye concentrations at different intervals of time. The straight line represents the linear fitting of experimental dye degradation data for kinetic interpretation. It was observed from the graph plot that data rarely follow a straight line. This pattern shows that dye degradation does not follow zero-order reaction kinetics Chandekar et al. 2023).

Figure 13b graph is plotted between time on the x-axis and ln[dye] along the y-axis to determine the order for the dye degradation by using active catalytic grains following the linear data fitting model. Similarly, Fig. 13c represents the graph between time and 1/ln[dye] to check dye degradation order against the catalyst used for the reaction. The R^2 values for zero, first, and second order were found to be 0.8458, 0.9857, and 0.9556, respectively, as shown in the graph. The highest R^2 values obtained in Fig. 11b represent that dye decolorization reaction using active catalyst follows first-order reaction kinetics.

Dye degradation study

Azo dye is a big class of dyes, and Reactive Red 195 belongs to it. In the degradation of dye firstly, the azo bond breaks down as displayed in the figure given below (Fig. 14). Then, desulfonation and deamination took place. CO_2, SO_2, NO_3^{-1}, NH_4^+, etc., are end products (David et al. 2020; Gola et al. 2021). The adsorption method and accelerated dye degradation are the basic probable methods for encapsulated nanoparticles. Electron transport might be used to explain the decolorization reactions. The potential of the substances to provide electrons and the dye molecule's aptitude to receive them are strongly related to the catalytic activity of the encapsulated MgO NPs. The dye is firstly affixed to the encapsulated MgO NPs' face. Following sorption, the capping reagent made of polyphenolic substances functions as a potent nucleophilic substance, while the dye component functions as an electrophilic reagent (Yu et al. 2022). The MgO NPs in a solution serve as a conduit, transporting the electrons needed for the dye molecules to be destroyed from

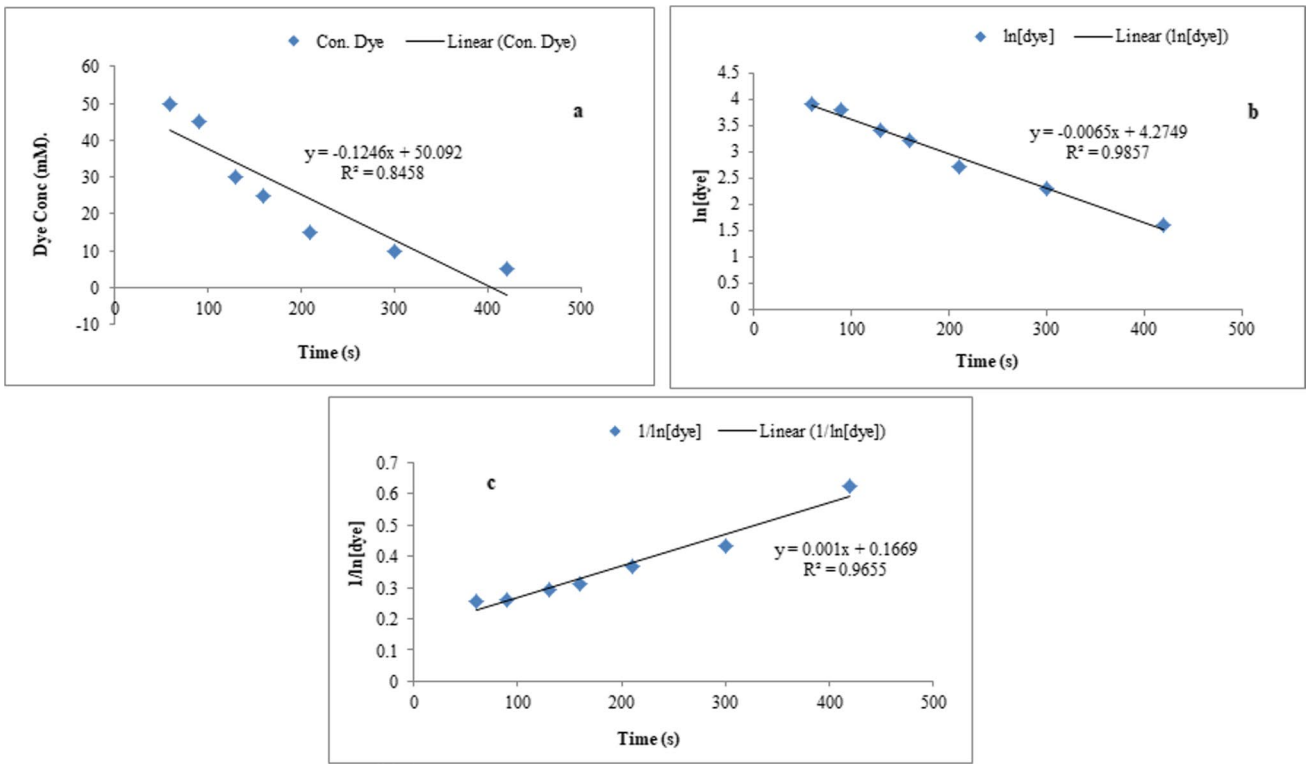

Fig. 13 Absorbance data fitting of Reactive Red 195 dye reduction carried out by MgO NPs catalyst to the (**a**) zero-, (**b**) first-, and (**c**) second-order reaction kinetics

the capping reagent to the dye molecule (Venkataravanappa et al. 2018; Kale et al. 2018; Raza et al. 2020).

Catalyst reusability

After every reaction round, the catalyst was separated and reused using the same procedure. 91–87% of the reaction's efficiency was produced without problems (Table 2). According to the outcome, the catalyst's effectiveness was not significantly impacted by reuse. Recyclability is essential when assessing catalytic effectiveness (Kalaiarasan et al. 2021). The MgO catalyst can be seen to exhibit 90% degradation in each of the five phases, demonstrating the chemically stable nature of the synthesized catalyst in an aqueous solution (Vishakar et al. 2021; Chandekar et al. 2023). As evidence of the chemically stable nature of MgO NPs (prepared via a biogenic way using water as a solvent), our investigation's catalyst reusability for 4 cycles stayed at 87%.

Practical/Future implications of the study

The entire research was conducted in a laboratory, where *Azadirachta indica* leaf extract was used to create MgO nanoparticles, which were then used to accelerate the breakdown of the Reactive Red 195 dye. This laboratory work can be applied on a large scale for the wastewater treatment of industrial dyes. With the uses of this study work, we can eliminate not merely green waste but effluent that may be processed as well inexpensively and water that could be employed for various uses without having to go through costly treatment methods.

Conclusion

Green synthesis of nanoparticles is being made possible by the rapid rise in awareness of less hazardous, sustainable, and environmentally friendly approaches. Because plant extracts are rich in reducing and capping agents, the number of chemicals needed to make metal oxide nanoparticles was minimized. Neem (*Azadirachta indica*) leaves aqueous extract synthesized MgO NPs. The produced nanoparticles have a cubic structure, are crystalline, and have a size of

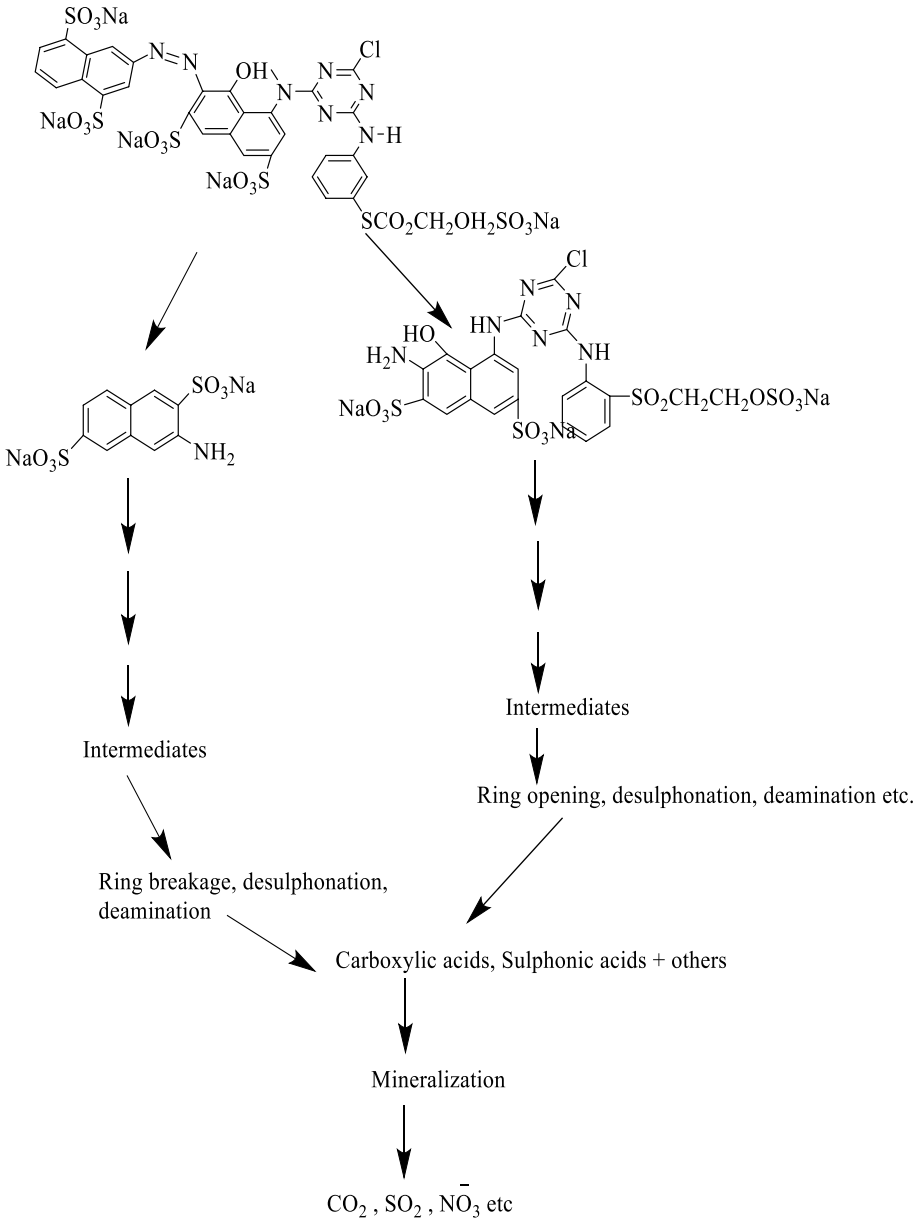

Fig. 14 Proposed degradation pathway of RR-195 dye

Table 2 Investigation of the recyclability of the catalyst

Recycle time	1	2	3	4
Yield (%)	91%	90%	88%	87%

about 60 nm. The Mg-O bond's existence was verified by FTIR analysis. The generated nanoparticles' cluster shape is shown via surface examination. Additionally, synthetic MgO NPs were utilized to confiscate the renowned Reactive Red 195 dye used in many textile processes. Parameters were optimized by examining the effects of temperature, pH, dye concentration, and NP content. The highest decolorization was at 0.02% concentration, pH 4, 40 °C temperature, and 0.003 g/L catalyst dosage. TOC and COD levels have been found to have decreased by 84.33% and 81.3%, respectively. The degradation of our dye was 87% when the catalyst was recycled up to four times. The target dye's decomposition process led to the production of less toxic and simpler related chemicals. MgO NPs are a promising catalyst due to their wide application, ease of handling, workability, and better yields. In light of this, it can be inferred that MgO nanoparticles made using a greener process could be utilized as a magnetic catalyst to break down other dyes. The toxic effects of synthetic dyes in wastewater can be reduced by using these MgO nanoparticles to remove other synthetic dyes.

Acknowledgements The authors are thankful to the Deanship of Scientific Research at Najran University for funding this work under the Research Groups Funding Program grant code (NU/RG/SERC/12/4), and Department of Applied Chemistry, Government College University, Faisalabad, Pakistan, for providing the necessary facilities to carry out this study.

Funding This authors are thankful to the Deanship of Scientific Research at Najran University for funding this work under the Research Groups Funding Program grant code (NU/RG/SERC/12/4).

Data availability All the data relevant to this study are mentioned in the manuscript. There are no supplementary data.

Declarations

Competing interests The authors declare no financial or competing interest.

Human and animal rights This study followed the ethical standards. It involves not human or animal-based study.

References

Abdulkhaleq NA, Nayef UM, Albarazanchi K (2020) MgO nanoparticles synthesis via laser ablation stationed on porous silicon for photoconversion application. Optik 212:164793. https://doi.org/10.1016/j.ijleo.2020.164793

Ahuja N, Chopra AK, Ansari AA (2016) Removal of colour from aqueous solutions by using zero valent iron nanoparticles. J Environ Sci Toxicol Food Technol 10(1):4–14. https://doi.org/10.9790/2402-10120414

Anumol EA, Kundu P, Deshpande PA, Madras G, Ravishankar N (2011) New insights into selective heterogeneous nucleation of metal nanoparticles on oxides by microwave-assisted reduction: rapid synthesis of high-activity supported catalysts. ACS Nano 5(10):8049–8061. https://doi.org/10.1021/nn202639f

Aqeel M, Ikram M, Asghar A, Haider A, Ul-Hamid A, Naz M, Imran M, Ali S (2020) Synthesis of capped Cr-doped ZnS nanoparticles with improved bactericidal and catalytic properties to treat polluted water. Appl Nanosci 10(6):2045–2055. https://doi.org/10.1007/s13204-020-01268-3

Aravind P, Selvaraj H, Ferro S, Sundaram M (2016) An integrated (electro-and bio-oxidation) approach for remediation of industrial wastewater containing azo-dyes: understanding the degradation mechanism and toxicity assessment. J Hazard Mater 318:203–215. https://doi.org/10.1016/j.jhazmat.2016.07.028

Asefi D, Mahmoodi NM, Arami M (2010) Effect of nonionic co-surfactants on corrosion inhibition effect of cationic gemini surfactant. Colloids Surf A Phys Chem Eng Asp 355(1–3):183–186. https://doi.org/10.1016/j.colsurfa.2009.12.019

Aziz A, Memon Z, Bhutto A (2023) Efficient photocatalytic degradation of industrial wastewater dye by *Grewia asiatica* mediated zinc oxide nanoparticles. Optik 272:170352. https://doi.org/10.1016/j.ijleo.2022.170352

Baharfar R, Shariati N (2014) An efficient one-pot synthesis of novel isatin-based 2-amino thiazol-4-one conjugates using MgO nanoparticles in aqueous media. C R Chim 17(5):413–419. https://doi.org/10.1016/j.crci.2013.08.010

Bhatti HN, Akram N, Asgher M (2008) Optimization of culture conditions for enhanced decolorization of Cibacron Red FN-2BL by *Schizophyllum commune* IBL-6. J Appl Biochem Biotechnol 149:255–264. https://doi.org/10.1007/s12010-007-8123-x

Bhuiyan MR, Rahman MM, Shaid A, Bashar MM, Khan MA (2016) Scope of reusing and recycling the textile wastewater after treatment with gamma radiation. J Cleaner Prod 112:3063–3071. https://doi.org/10.1016/j.jclepro.2015.10.029

Buazar F, Bavi M, Kroushawi F, Halvani M, Khaledi-Nasab A, Hossieni SA (2016) Potato extract as reducing agent and stabiliser in a facile green one-step synthesis of ZnO nanoparticles. J Exper Nanosci 11(3):175–184. https://doi.org/10.1080/17458080.2015.1039610

Chandekar KV, Palanivel B, Alkallas FH, Trabelsi ABG, Khan A, Ashraf IM, Alfaifay S, Shkir M (2023) Photocatalytic activities of Mg doped NiO NPs for degradation of Methylene blue dye for harmful contaminants: a kinetics, mechanism and recyclability. J Physics Chem Solids 178:111345. https://doi.org/10.1016/j.jpcs.2023.111345

Chen D, Zhang C, Rong H, Zhao M, Gou S (2020) Treatment of electroplating wastewater using the freezing method. Separ Purif Technol 234:116043. https://doi.org/10.1016/j.seppur.2019.116043

da Silva BC, Zanutto A, Pietrobelli JM (2019) Biosorption of reactive yellow dye by malt bagasse. Adsorp Sci Technol 37(3–4):236–259. https://doi.org/10.1177/0263617418823995

David L, Moldovan B (2020) Green synthesis of biogenic silver nanoparticles for efficient catalytic removal of harmful organic dyes. Nanomater 10(2):202. https://doi.org/10.3390/nano10020202

Di DR, He ZZ, Sun ZQ, Liu J (2012) A new nano-cryosurgical modality for tumor treatment using biodegradable MgO nanoparticles. Nanomed Nanotechnol Biol Med 8(8):1233–1241. https://doi.org/10.1016/j.nano.2012.02.010

Durán N, Marcato PD, Durán M, Yadav A, Gade A, Rai M (2011) Mechanistic aspects in the biogenic synthesis of extracellular metal nanoparticles by peptides, bacteria, fungi, and plants. Appl Microbiol Biotechnol 90(5):1609–1624. https://doi.org/10.1007/s00253-011-3249-8

Elashery SE, Ibrahim I, Gomaa H, El-Bouraie MM, Moneam IA, Fekry SS, Mohamed GG (2023) Comparative study of the photocatalytic degradation of crystal violet using ferromagnetic magnesium oxide nanoparticles and MgO-bentonite nanocomposite. Magnetochem 9(2):56. https://doi.org/10.3390/magnetochemistry9020056

Elumalai K, Velmurugan S (2015) Green synthesis, characterization and antimicrobial activities of zinc oxide nanoparticles from the leaf extract of *Azadirachta indica* (*L.*). Appl Surf Sci 345:329–336. https://doi.org/10.1016/j.apsusc.2015.03.176

Fakhri A, Adami S (2014) Adsorption and thermodynamic study of Cephalosporins antibiotics from aqueous solution onto MgO nanoparticles. J Taiwan Inst Chem Eng 45(3):1001–1006. https://doi.org/10.1016/j.jtice.2013.09.028

Foster SL, Estoque K, Voecks M, Rentz N, Greenlee LF (2019) Removal of synthetic azo dye using bimetallic nickel-iron nanoparticles. J Nanomater 9807605:1–12. https://doi.org/10.1155/2019/9807605

Fouda A, Awad MA, Eid AM, Saied E, Barghoth MG, Hamza MF, Awad MF, Abdelbary S, Hassan SED (2021) An eco-friendly approach to the control of pathogenic microbes and *Anopheles stephensi* malarial vector using magnesium oxide nanoparticles (Mg-nps) fabricated by *Penicillium chrysogenum*. Int J Mole Sci 22(10):096. https://doi.org/10.3390/ijms22105096

Ghaffar A, Kiran S, Rafique MA, Iqbal S, Nosheen S, Hou Y, Aimun U (2021) *Citrus paradisi* fruit peel extract mediated green synthesis of copper nanoparticles for remediation of disperse yellow 125 dye. Desalin Water Treat 212(7):368–375. https://doi.org/10.5004/dwt.2021.26684

Gholizadeh BS, Buazar F, Hosseini SM, Mousavi SM (2018) Enhanced antibacterial activity, mechanical and physical properties of alginate/hydroxyapatite bionanocomposite film. Int J Biol Macromol 116:786–792. https://doi.org/10.1016/j.ijbiomac.2018.05.104

Gola D, Bhatt N, Bajpai M, Singh A, Arya A, Chauhan N, Srivastava SK, Tyagi PK, Agrawal Y (2021) Silver nanoparticles for enhanced dye degradation. Curr Res Green Sust Chem 4:100132. https://doi.org/10.1016/j.crgsc.2021.100132

Greenberg BL, 1985. Washington, DC: U.S. Patent and trademark office, U.S. Patent No. 4, 547:804.

Gulzar T, Huma T, Jalal F, Iqbal S, Abrar S, Kiran S, Rafique MA (2017) Bioremediation of synthetic and industrial effluents by *Aspergillus niger* isolated from contaminated soil following a sequential strategy. Molecules 22(12):2244. https://doi.org/10.3390/molecules22122244

Hube S, Eskafi M, Hrafnkelsdóttir KF, Bjarnadóttir B, Bjarnadóttir MÁ, Axelsdóttir S, Wu B (2020) Direct membrane filtration for wastewater treatment and resource recovery. A review. Sci Total Environ 710:136375. https://doi.org/10.1016/j.scitotenv.2019.136375

Ikram M, Imran M, Nunzi JM, Ali S (2015) Efficient inverted hybrid solar cells using both CuO and P3HT as an electron donor materials. J Mater Sci Mater Electron 26(9):6478–6483. https://doi.org/10.1007/s10854-015-3239-1

Ikram M, Abbasi S, Haider A, Naz S, Ul-Hamid A, Imran M, Haider J, Ghaffar A (2020) Bimetallic Ag/Cu incorporated into chemically exfoliated MoS_2 nanosheets to enhance its antibacterial potential: in silico molecular docking studies. Nanotechnol 31(27):275704. https://doi.org/10.1088/1361-6528/ab8087

Jaina S, Bhatt A, Baba SA, Bisht VS, Biswas P, Ambatipudi K, Navani NK (2023) Concurrent mitigation and facile monitoring of xenobiotics by a highly efficient and recyclable nanoengineered catalyst. Chem Eng J 89:145074. https://doi.org/10.1016/j.cej.2023.145074

Jindarom C, Meeyoo V, Kitiyanan B, Rirksomboon T, Rangsunvigit P (2007) Surface characterization and dye adsorptive capacities of char obtained from pyrolysis/gasification of sewage sludge. Chem Eng J 133(1–3):239–246. https://doi.org/10.1016/j.cej.2007.02.002

Kalaiarasan S, Uthirakumar P, Shin DY, Lee IH (2021) The degradation profile of high molecular weight textile reactive dyes: A daylight induced photocatalytic activity of ZnO/carbon quantum dot photocatalyst. Environ Nanotechnol Monitor Manage 15:100423. https://doi.org/10.1016/j.enmm.2020.100423

Kale RD, Kane PB (2018) Synthesis of PVP stabilized bimetallic nanoparticles for removal of azo based reactive dye from aqueous solution. Sust Chem Pharm 10:153–162. https://doi.org/10.1016/j.scp.2018.11.002

Kamranifar M, Khodadadi M, Samiei V, Dehdashti B, Sepehr MN, Rafati L, Nasseh N (2018) Comparison the removal of reactive red 195 dye using powder and ash of barberry stem as a low cost adsorbent from aqueous solutions: Isotherm and kinetic study. J Mol Liq 255:572–577. https://doi.org/10.1016/j.molliq.2018.01.188

Kandiban M, Vigneshwaran P, Potheher IV (2015) Synthesis and characterization of Mgo nanoparticles for photocatalytic applications. In Department of physics, bharathidasan institute of technology (BIT) campus, Anna University, Tiruchirappalli, Conference Paper.

Kargozar S, Mozafari M (2018) Nanotechnology and nanomedicine start small think big. Mater Today Proc 5(7):5492–15500. https://doi.org/10.1016/j.matpr.2018.04.155

Khalid NR, Ahmed E, Ikram M, Ahmad M, Phoenix DA, Elhissi A, Ahmed W, Jackson MJ (2013) Effects of calcination on structural, photocatalytic properties of TiO_2 nanopowders via $TiCl_4$ hydrolysis. J Mater Eng Perform 22(2):371–375. https://doi.org/10.1007/s11665-012-0272-6

Khalil A, Ali N, Asiri AM, Kamal T, Khan SB, Ali J (2021) Synthesis and catalytic evaluation of silver nickel oxide and alginate biopolymer nanocomposite hydrogel beads. Cellulose 28:11299–11313. https://doi.org/10.1007/s10570-021-04248-0

Khandaker NR, Afreen I, Huq FB, Akter T (2010) Treatment of textile wastewater using calcium hypochlorite oxidation followed by waste iron rust aided rapid filtration for color and COD removal for application in resources challenged Bangladesh. Groundw Sust Dev 10:100342. https://doi.org/10.1016/j.gsd.2020.100342

Kiran S, Adeel S, Nosheen S, Hassan A, Usman M, Rafique MA (2017) Recent trends in textile effluent treatments—a review. Adv Mater Wastewater Treat 29:29–49

Kiran S, Rafique MA, Iqbal S, Nosheen S, Naz S, Rasheed A (2020) Synthesis of nickel nanoparticles using *Citrullus colocynthis* stem extract for remediation of reactive yellow 160 dye. Environ Sci Poll Res 27(26):32998–33007. https://doi.org/10.1007/s11356-020-09510-9

Kiran S, Nosheen S, Iqbal S, Abrar S, Jalal F, Gulzar T, Naseer N (2018) Photocatalysis using titanium dioxide for treatment of textile wastewater containing disperse dyes. Chiang Mai J Sci 45:2730–2739. http://epg.science.cmu.ac.th/ejournal/

Kumar KM, Mandal BK, Kumar KS, Reddy PS, Sreedhar B (2013) Biobased green method to synthesise palladium and iron nanoparticles using *Terminalia chebula* aqueous extract. Spectrochim Acta A Mol Biomol Spectrosc 102:128–133. https://doi.org/10.1016/j.saa.2012.10.015

Lafta AJ (2015) Effect of activation temperature on ability of activated carbon on removal of reactive yellow 145 dye from simulated industrial textile wastewaters. J Chem Pharm Res 7(11):158–169

Leyla CE, Ayten OZR, Meysun IA (2012) Biodegradation of reactive red 195 azo dye by the bacterium *Rhodopseudomonas palustris* 51ATA. Afr J Microbiol Res 6(1):120–126. https://doi.org/10.5897/AJMR11.1059

Li X, Huang X, Zhao C, Wang X, Dong B, Goonetilleke A, Kim K (2023) Characterizing molecular transformation of dissolved organic matter during high-solid anaerobic digestion of dewatered sludge using ESI FT-ICR MS. Chemosphere 320:138101. https://doi.org/10.1016/j.chemosphere.2023.138101

Lourens A, Falch A, Malgas-Enus R (2023) Magnetite immobilized metal nanoparticles in the treatment and removal of pollutants from wastewater: a review. J Mater Sci 58(7):2951–2970. https://doi.org/10.1007/s10853-023-08167-2

Mahmoodi NM (2013a) Photodegradation of dyes using multiwalled carbon nanotube and ferrous ion. J Environ Eng 139(11):1368–1374. https://doi.org/10.1061/(ASCE)EE.1943-7870.0000762

Mahmoodi NM (2013b) Synthesis of amine-functionalized magnetic ferrite nanoparticle and its dye removal ability. J Environ Eng 139:1382–1390. https://doi.org/10.1061/(ASCE)EE.1943-7870.0000763

Mahmoodi NM (2014) Synthesis of core–shell magnetic adsorbent nanoparticle and selectivity analysis for binary system dye removal. J Ind Eng Chem 20(4):2050–2058. https://doi.org/10.1016/j.jiec.2013.09.030

Mahmoodi NM (2015) Manganese ferrite nanoparticle: synthesis, characterization, and photocatalytic dye degradation ability. Desalin Water Treat 53(1):84–90. https://doi.org/10.1080/19443994.2013.834519

Mahmoodi NM, Limaee NY, Arami M, Borhany S, Mohammad-Taheri M (2007) Nanophotocatalysis using nanoparticles of titania: mineralization and finite element modelling of Solophenyl dye decolorization. J Photochem Photobiol A Chem 189(1):1–6. https://doi.org/10.1016/j.jphotochem.2006.12.025

Mahmoodi NM, Hayati B, Arami M (2010) Textile dye removal from single and ternary systems using date stones: kinetic, isotherm, and thermodynamic studies. J Chem Eng Data 55(11):4638–4649. https://doi.org/10.1021/je1002384

Mahmoodi NM, Taghizadeh M, Taghizadeh A (2018) Mesoporous activated carbons of low-cost agricultural bio-wastes with high adsorption capacity: preparation and artificial neural network modeling of dye removal from single and multicomponent (binary and ternary) systems. J Mol Liq 269:217–228. https://doi.org/10.1016/j.molliq.2018.07.108

Mahmoodi NM, Taghizadeh M, Taghizadeh A (2019) Activated carbon/metal-organic framework composite as a bio-based novel green adsorbent: preparation and mathematical pollutant removal modeling. J Mol Liq 277:310–322. https://doi.org/10.1016/j.molliq.2018.12.050

Makarov VV, Love AJ, Sinitsyna OV, Makarova SS, Yaminsky IV, Taliansky ME, Kalinina NO (2014) Green nanotechnologies synthesis of metal nanoparticles using plants. Acta Naturae 6(20):35–44

Moavi J, Buazar F, Sayahi MH (2021) Algal magnetic nickel oxide nanocatalyst in accelerated synthesis of pyridopyrimidine derivatives. Sci Rep 11(1):1–14. https://doi.org/10.1038/s41598-021-85832-z

Mohammad EJ, Lafta AJ, Kahdim SH (2016) Photocatalytic removal of reactive yellow 145 dye from simulated textile wastewaters over supported (Co, Ni)3_4/Al2_3 co-catalyst. Pol J Chem Technol 18(3):1–9. https://doi.org/10.1515/pjct-2016-0041

Moorthy SK, Ashok CH, Rao KV, Viswanathan C (2015) Synthesis and characterization of MgO nanoparticles by Neem leaves through green method. Mater Today Proc 2(9):4360–4368. https://doi.org/10.1016/j.matpr.2015.10.027

Nabi G, Ain QU, Tahir MB, Nadeem RK, Iqbal T, Rafique M, Hussain S, Raza W, Aslam I, Rizwan M (2022) Green synthesis of TiO_2 nanoparticles using lemon peel extract: their optical and photocatalytic properties. Int J Environ Anal Chem 102(2):434–442. https://doi.org/10.1080/03067319.2020.1722816

Naseer A, Nosheen S, Kiran S, Kamal S, Javaid MA, Mustafa M, Tahir A (2016) Degradation and detoxification of Navy Blue CBF dye by native bacterial communities: an environmental bioremedial approach. Desalin Water Treat 57(50):4070–24082. https://doi.org/10.1080/19443994.2016.1138145

Nezhadheydari H, Tavabe KR, Mirvaghefi A, Heydari A, Frinsko M (2019) Effects of different concentrations of Fe_3O_4@ ZnO and Fe_3O_4@ CNT magnetic nanoparticles separately and in combination on aquaculture wastewater treatment. Environ Technol Innov 15:100414. https://doi.org/10.1016/j.eti.2019.100414

Nga NK, Hong PTT, Dai LT, Huy TQ (2013) A facile synthesis of nanostructured magnesium oxide particles for enhanced adsorption performance in reactive blue 19 removal. J Coll Inter Sci 398:210–216. https://doi.org/10.1016/j.jcis.2013.02.018

Nguyen DTC, Dang HH, Vo DVN, Bach LG, Nguyen TD, Tran TV (2021) Biogenic synthesis of MgO nanoparticles from different extracts (flower, bark, leaf) of *Tecoma stans* (L.) and their utilization in selected organic dyes treatment. J Hazard Mater 404:124146. https://doi.org/10.1016/j.jhazmat.2020.124146

Pang S, Zhou C, Sun Y, Zhang K, Ye W, Zhao X, Hui B (2023) Natural wood-derived charcoal embedded with bimetallic iron/cobalt sites to promote ciprofloxacin degradation. J Clean Prod 414:137569. https://doi.org/10.1016/j.jclepro.2023.137569

Patil SP, Chaudhari RY, Nemade MS (2022) *Azadirachta indica* leaves mediated green synthesis of metal oxide nanoparticles. A review. Talanta Open 59:100083. https://doi.org/10.1016/j.talo.2022.100083

Prabhu PS, Kathirvel P, Maruthamani D, Ram SG (2023) Enhanced photocatalytic activity of methylene blue dye by DIFS synthesized pure and Mn doped MgO nanostructures. Optik 283:170869. https://doi.org/10.1016/j.ijleo.2023.170869

Rafique M, Shaikh AJ, Rasheed R, Tahir MB, Gillani SSA, Usman A, Imran M, Zakir A, Khan ZUH, Rabbani F (2018) Aquatic biodegradation of methylene blue by copper oxide nanoparticles synthesized from *Azadirachta indica* leaves extract. J Inorg Organom Polym Mater 28(6):2455–2462. https://doi.org/10.1007/s10904-018-0921-9

Rafique MA, Kiran S, Javed S, Ahmad I, Yousaf S, Iqbal N, Rani F (2021) Green synthesis of nickel oxide nanoparticles using *Allium cepa* peels for degradation of Congo red direct dye: an environmental remedial approach. Water Sci Technol 84(10–11):2793–2804. https://doi.org/10.2166/wst.2021.237

Rafique MA, Jamal A, Ali Z, Kiran S, Iqbal S, Nosheen S, Ansar Z, Hossain MB (2022) Biologically synthesized copper nanoparticles show considerable degradation of reactive red 81 dye: an eco-friendly sustainable approach. Bio Med Res Int 7537955:1–9. https://doi.org/10.1155/2022/7537955

Rasool A, Kiran S, Gulzar T, Abrar S, Ghaffar A, Shahid M, Nosheen S, Naz S (2023) Biogenic synthesis and characterization of ZnO nanoparticles for degradation of synthetic dyes: a sustainable environmental cleaner approach. J Clean Prod 398:136616. https://doi.org/10.1016/j.jclepro.2023.136616

Raza A, Qumar U, Hassan J, Ikram M, Ul-Hamid A, Haider J, Imran M, Ali S (2020) A comparative study of dirac 2D materials, TMDCs and 2D insulators with regard to their structures and photocatalytic/sonophotocatalytic behavior. Appl Nanosci 10(10):3875–3899. https://doi.org/10.1007/s13204-020-01475-y

Revathi T, Thambidurai S (2018) Immobilization of ZnO on Chitosan-neem seed composite for enhanced thermal and antibacterial activity. Adv Powder Technol 29(6):1445–1454. https://doi.org/10.1016/j.apt.2018.03.007

Rezaee A, Taghi GM, Jamalodin HS, Moussavi G, Khavanin A, Ghanizadeh G (2008) Decolorization of reactive blue 19 dye from textile wastewater by the UV/H_2O_2 process. J Appl Sci 8(6):1108–1112. https://doi.org/10.3923/jas.2008.1108.1112

Rezazadeh NH, Buazar F, Matroodi S (2020) Synergistic effects of combinatorial chitosan and polyphenol biomolecules on enhanced antibacterial activity of biofunctionalized silver nanoparticles. Sci Rep 10(1):1–13. https://doi.org/10.1038/s41598-020-76726-7

Roy P, Das B, Mohanty A, Mohapatra S (2017) Green synthesis of silver nanoparticles using *Azadirachta indica* leaf extract and its antimicrobial study. Appl Nanosci 7(8):843–850. https://doi.org/10.1007/s13204-017-0621-8

Safaei GJ, Zahedi S, Javid M, Ghasemzadeh MA (2015) MgO nanoparticles: an efficient, green and reusable catalyst for the onepot syntheses of 2, 6-dicyanoanilines and 1, 3-diarylpropyl malononitriles under different conditions. J Nanostr 5:153–160

Saied E, Eid AM, Hassan SED, Salem SS, Radwan AA, Halawa M, Saleh FM, Saad HA, Saied EM, Fouda A (2021) The catalytic activity of biosynthesized magnesium oxide nanoparticles (MgO-nps) for inhibiting the growth of pathogenic microbes, tanning effluent treatment, and chromium ion removal. Catalysts 11(7):821. https://doi.org/10.3390/catal11070821

Sathish T, Mohanavel V, Arunkumar M, Rajan K, Soudagar MEM, Mujtaba MA, Salmen SH, Obaid SA, Fayaz H, Sivakumar S (2022) Utilization of *Azadirachta indica* biodiesel, ethanol and diesel blends for diesel engine applications with engine emission profile. Fuel 319:123798. https://doi.org/10.1016/j.fuel.2022.123798

Sattar U, Ikram M, Junaid M, Aqeel M, Imran M, Ali S (2010) Annealing effect on synthesized ZnS/TiO_2 nanocomposite for treatment of industrial wastewater. Mater Res Express 6(11):115050. https://doi.org/10.1088/2053-1591/ab476c/meta

Sela SK, Nayab-Ul-Hossain AKM, Hussain SZ, Hasan N (2020) Utilization of prawn to reduce the value of BOD and COD of textile wastewater. Clean Eng Technol 1:100021. https://doi.org/10.1016/j.clet.2020.100021

Sepahvand M, Buazar F, Sayahi MH (2020) Novel marine-based gold nanocatalyst in solvent-free synthesis of polyhydroquinoline derivatives green and sustainable protocol. Appl Organom Chem 34(12):e6000. https://doi.org/10.1002/aoc.6000

Shah VB, Henson WR, Chadha TS, Lakin G, Liu H, Blankenship RE, Biswas P (2015) Linker-free deposition and adhesion of photosystem I onto nanostructured TiO_2 for biohybrid photoelectrochemical cells. Langmuir 31(5):1675–1682. https://doi.org/10.1021/la503776b

Sofi AH, Akhoon SA, Mir JF, Rather MUD (2021) Magnesium oxide (MgO) a viable agent for antimicrobial activity. In applications of nanomaterials in agriculture food science and medicine. IGI Global 58:98–105. https://doi.org/10.4018/978-1-7998-5563-7.ch005

Sun X, Chen Z, Sun Z, Wu S, Guo K, Dong Z, Peng Y (2023) High-Efficiency utilization of waste shield slurry: a geopolymeric flocculation-filtration-solidification method. Constr Build Mater 387:131569. https://doi.org/10.1016/j.conbuildmat.2023.131569

Tahir MY, Sillanpaa M, Almutairi TM, Mohammed AA, Ali S (2023) Excellent photocatalytic and antibacterial activities of bio-activated carbon decorated magnesium oxide nanoparticles. Chemosphere 312:137327. https://doi.org/10.1016/j.chemosphere.2022.137327

Tyagi S, Rawtani D, Khatri N, Tharmavaram M (2018) Strategies for nitrate removal from aqueous environment using nanotechnology a review. J Water Process Eng 21:84–95. https://doi.org/10.1016/j.jwpe.2017.12.005

Vaiano V, Iervolino G (2018) Facile method to immobilize ZnO particles on glass spheres for the photocatalytic treatment of tannery wastewater. J Colloid Interf Sci 518:192–199. https://doi.org/10.1016/j.jcis.2018.02.033

Venkataravanappa V, Ashwathappa KV, Hemachandra-Reddy P, Reddy CL, Jalali S, Reddy MK (2018) *Candidatus phytoplasma* belonging to the 16SrVI phytoplasma group, is associated with witches broom disease of *Azadirachta indica* in India. Aust Plant Dis Notes 13(1):1–4. https://doi.org/10.1007/s13314-018-0313-6

Verma A, Mehata MS (2016) Controllable synthesis of silver nanoparticles using neem leaves and their antimicrobial activity. J Radiat Res Appl Sci 9(1):109–115. https://doi.org/10.1016/j.jrras.2015.11.001

Vishakar VV, Vidya C, Hariharan N, Mohamed MA (2021) Investigational study on microbial degradation of reactive dye by using mixed consortium in the environment. Mater Today Proc 43:2036–2039. https://doi.org/10.1016/j.matpr.2020.11.792

Wang Z, Liu X, Ni S, Zhuang X, Lee T (2021) Nano zero-valent iron improves anammox activity by promoting the activity of quorum sensing system. Water Res 202:117491. https://doi.org/10.1016/j.watres.2021.117491

Wang Z, Hu L, Zhao M, Dai L, Hrynsphan D, Tatsiana S, Chen J (2022) Bamboo charcoal fused with polyurethane foam for efficiently removing organic solvents from wastewater: experimental and simulation. Biochar 4(1):28. https://doi.org/10.1007/s42773-022-00153-2

Yan R, Luo D, Fu C, Wang Y, Zhang H, Wu P, Jiang W (2020) Harmless treatment and selective recovery of acidic Cu (II)-Cr (VI) hybrid wastewater via coupled photo-reduction and ion exchange. Sep Purif Technol 234:116130. https://doi.org/10.1016/j.seppur.2019.116130

Yaseen DA, Scholz M (2019) Textile dye wastewater characteristics and constituents of synthetic effluents: a critical review. Int J Environ Sci Technol 16:1193–1226. https://doi.org/10.1007/s13762-018-2130-z

Yu K, Sun C, Zhang B, Hassan M, Hassan M, He Y (2019) Size-dependent adsorption of antibiotics onto nanoparticles in a field-scale wastewater treatment plant. Environ Pollut 248:1079–1087. https://doi.org/10.1016/j.envpol.2019.02.090

Yu H, Zhu J, Qiao R, Zhao N, Zhao M, Kong L (2022) Facile preparation and controllable absorption of a composite based on PMo12/Ag nanoparticles: photodegradation activity and mechanism. Chem Select 7(2):e202103668. https://doi.org/10.1002/slct.202103668

Zhang J, Zhong A, Huang G, Yang M, Li D, Teng M, Han D (2020) Enhanced efficiency with CDCA co-adsorption for dye-sensitized solar cells based on metallosalophen complexes. Sol Energy 209:316–324. https://doi.org/10.1016/j.solener.2020.08.096

Zhao J, Zhang B, Zuo J (2019) Response of anammox granules to ZnO nanoparticles at ambient temperature. Environ Technol Innov 13:146–152. https://doi.org/10.1016/j.eti.2018.11.002

Zhou H, Wei C, Zhang F, Hu Y, Wu H, Kraslawski A (2019) A comprehensive evaluation method for sludge pyrolysis and adsorption process in the treatment of coking wastewater. J Environ Manag 235:423–431. https://doi.org/10.1016/j.jenvman.2019.01.093